13th ewtec 2019
Proceedings of the 13th European Wave and Tidal Energy Conference 1-6 Sept 2019, Naples, Italy

Mooring system reliability analysis of an ORE device using general Polynomial Chaos

Guilherme Moura Paredes, Jonas Bjerg Thomsen, Francesco Ferri and Claes Eskilsson

***Abstract*—We demonstrate the use of *general Polynomial Chaos* (gPC) in determining the reliability of a mooring system designed for an offshore renewable energy (ORE) device. General Polynomial Chaos is used to forward propagate uncertainties in two design variables, and to obtain the probability density function of the Most Probable Maximum tension in the most loaded line. Then, the probability of failure is estimated using the First Order Reliability Method. For this case study, we obtain a probability of failure of 3.4×10^{-6} for the mooring system, around 10 times lower than required by DNV-OS-E301. The most interesting result, however, is that by applying gPC, we can build a probability density function for the tension running only 36 simulations using the deterministic numerical model, instead of hundreds or thousands as would be required by using a Monte Carlo method. This reduces the computational effort required for probabilistic design and analysis of floating structures, enabling the shift from conservative Partial Safety Factor based design, to Reliability and Risk based design.**

***Index Terms*—Reliability, mooring systems, general Polynomial Chaos, stochastic collocation method, floating renewable energy systems, offshore renewable energy.**

I. Introduction

DETERMINISTIC design, the standard structural design method, is appealing for its ease and fast application, as well as for its intuitive nature. In any of its different forms, the goal is to ensure that a characteristic extreme load acting on a structure, multiplied by a factor greater than 1, is smaller than strength of the structure, divided by a factor greater than 1. The determination of the characteristic load and strength, as well as the so-called safety factors to use, are tabulated in design regulations. However, despite its attractiveness, deterministic design has important drawbacks [1]: first it is only acceptable in situations where there is an extensive database of designed cases that can be used to calibrate the safety factors; second, it does not guarantee that for all the structural elements, or, even across a single structural element, the probability of failure is kept constant. This can lead to both over- and under-designed situations, neither of which is desired.

Mooring systems are often designed using the Deterministic approach, following regulations, such as DNV-OS-E301 [2], which recommend safety factors that should guarantee no more than one cable failure in 10 000 years of operation. However, this is far from being true. As reported by Bindley and Comley [3], in the UK Continental Shelf, the failure rates of mooring cables are 1 every 24 years, for single cables, and 1 every 112 years for multiple cables. This is around 1000 times higher than expected in mooring design standards. Moreover, increasing the strength of mooring cables does not seem to increase their reliability: even platforms with higher design strength requirements for mooring cables yield similar failure rates [3]. This shows the need for improved design procedures and consideration of different failure mechanisms.

In reliability based design, both the load and the resistance are characterised by their statistical distributions, instead of deterministic values. As stated in [4]:

> *The main objective of structural design is, therefore, to ensure, at an acceptable level of probability, that each structure will not become unfit for its intended purpose at any time during its specified design life.*

Reliability based design is more involved than the deterministic design, but it is effective in the economic and safe design of uncommon structures and critical components. It can also account for uncertainties in the design, manufacture, construction, and installation of the components and structure, in a scientifically rigorous way.

Offshore renewable energy converters (OREC) are far from being standard structures: there are too few cases deployed to have enough information to calibrate safety factors; and information on the typical failure modes is still unknown. The high cost of the mooring system has partly contributed to low economic viability of investments in floating renewable energy technology. To ease the costs of development, some prototypes have been deployed with improperly designed mooring systems, which later failed, resulting in the loss of the prototype [5]. All these reasons point to Reliability-based design being a good approach to design mooring systems for offshore renewable energy devices. And that is why we will preform a reliability analysis of a mooring system.

The mooring system analysed in the present study, described in section III, is designed using the Floating

Paper no: 1271. Part of track: Station-keeping, mooring and foundations. This work received funding from the European Union's Horizon 2020 research and innovation programme under grant agreement No. 752031 for project *MoWE–Mooring of floating wave energy converters: numerical simulation and uncertainty quantification* and from the Energy Technology Development and Demonstration Program (EUDP) through the project *Mooring Solutions for Large Wave Energy Converters* (Grant Number 64014-0139).

The authors are all with the Department of Civil Enginering, Aalborg University, DK-9220 Aalborg Ø, Denmark.
G. Moura Paredes (gmp@civil.aau.dk).
J. Bjerg Thomsen (jbt@civil.aau.dk).
F. Ferri (ff@civil.aau.dk).
C. Eskilsson (cge@civil.aau.dk).

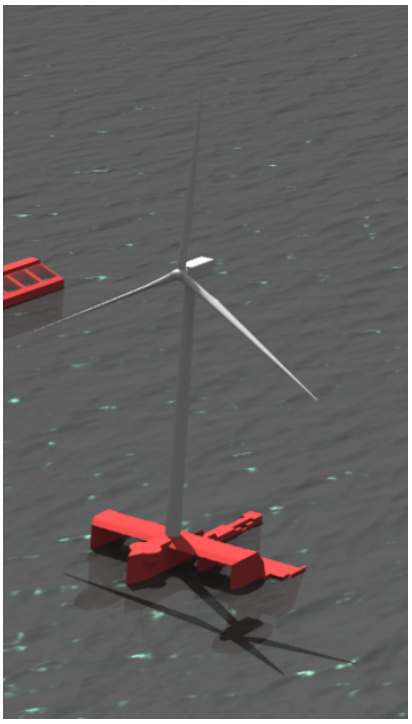

Fig. 1. Illustration of the Floating Power Plant P60. Adapted from [7]

Power Plant (FPP) hybrid offshore renewable energy converter [6] as example, see Fig. 1. The mooring was designed in the Mooring Solutions for Large Wave Energy Converters (MSLWEC) project [6] and used as a test case for investigating mooring systems for large wave energy converters. We stress that the mooring system used in the present study does not resemble the final mooring design for the FPP P60 device. The system was designed using a deterministic method, based on safety factors.

The goal of our analysis, presented in section IV, is to obtain the probability of failure of the mooring system, using the first order reliability method, and compare it with the reliability requirements of the standard DNV-OS-E301: Position Mooring [2]. We will account for uncertainties in both environmental and material parameters: water depth, cable stiffness, and cable strength. The response of the OREC for different input values of the uncertain parameters is computed in OrcaFlex, described in section II-B. In our case, the quantity of interest is the Most Probable Maximum (MPM) tension in the cables, for a range of values of rope stiffness and water depth.

Instead of the usual approach, based on the Monte Carlo Method, to aid in the task of Reliability Design and Analysis, we propose an approach based on (gPC). General Polynomial Chaos [8], described in section II-C, provides surrogate models for processes with random inputs, based on polynomial expansions. Compared with a PDE-deterministic model, a gPC model has two significant advantages. First, for the same inputs, gPC models are almost always faster to evaluate; second, the mean and variance of the PDE-model with random inputs are encoded in the polynomial coefficients of the gPC expansion. These properties make gPC a practical tool for the forward propagation of uncertainty, which is essential in reliability analysis: we are able to quickly obtain the probability density and distribution functions of complex processes, by running a very large number of input samples through the gPC model rather than through the PDE one. A first application of gPC to study mooring systems is presented in [9], about the influence of uncertainty in the hydrodynamic coefficients of mooring cables and anchor positions, in snap loads and dynamics of floating structures. General Polynomical Chaos is an established method and has been applied to other fields too. Some examples include the study of vehicle dynamics, [10], the performance of wind turbines [11], CFD simulations [12], wave propagation over random bathymetry [13], and to the study of a heaving cylinder in irregular waves [14].

The particular gPC formulation used, the Stochastic Collocation Method, is a non-intrusive method that requires only a few tens or hundreds of simulations of the deterministic PDE model, using specific points of the random sampling space. In contrast, a Monte Carlo method would require hundreds to thousands of simulations in the PDE model.

The analysis presented is simplified, in that only three parameters are judged to have uncertainties. However, it suffices to illustrate the method.

II. Theory and Methods

A. Reliability Analysis

A structure will fail if the load, L, acting on it is greater than the structure's strength, S. The limit criterion for failure is having the load equal to the strength, called the limit state function g [4]:

$$g = L - S = 0 \tag{1}$$

Reliability design and analysis looks at the probability of failure, P_{F}, of a structure or component, which is the probability that the strength is smaller than the load:

$$P_{\mathrm{F}} = P\left(S - L < 0\right) \tag{2}$$

For the case of where the load and the resistance are independent and normally distributed, the probability of failure will also be normally distributed, with mean value μ_{F} and standard deviation σ_{F} given by:

$$\mu_{\mathrm{F}} = \mu_S - \mu_L \tag{3a}$$

$$\sigma_{\mathrm{F}} = \sqrt{\sigma_S^2 + \sigma_L^2} \tag{3b}$$

where μ_S and σ_S are, respectively, the mean and the standard deviation of the strength of the component, and μ_L and σ_L, are, respectively, the mean and the standard deviation of the load. The probability of failure is then easily obtained by:

$$P_{\mathrm{F}} = \Phi\left(-\frac{\mu_{\mathrm{F}}}{\sigma_{\mathrm{F}}}\right) = \Phi\left(-\beta\right) \tag{4}$$

where Φ is the standard normal distribution function, and β is the reliability factor.

When the load or the resistance values are not normally distributed, they can be normalised using the

procedure described in [1]: first, the relevant side of the histogram of the quantities of interest is mirrored around the the modal value (the right side of the histogram for loads, and the left side of the histogram for strengths). In the new distribution, the modal value will also be be the mean, just as in a normal distribution. The normalised standard deviation is determined as the standard deviation of the new histogram; in other words, the values that were mirrored around the mode are accounted for twice. This procedure is also useful when there are only measurements of the values of the quantities of interest, but no analytical distribution that adequately fits them.

B. Hydrodynamic Model

The response analysis of the OREC and mooring is based on a numerical model using the open source boundary element method (BEM) code, Nemoh [15], and the commercial time domain solver OrcaFlex [16]. The current chapter briefly describes the numerical model, and more information can be found in [5], [17].

1) Numerical Model: The numerical model is based on a BEM code which solves the hydrodynamic coefficients using linear potential flow theory and a time domain solver, which solves all the environmental loads on the structure, and estimates the motion and mooring line response. The time domain solver, OrcaFlex, utilizes Cummin's Equation [18], to calculate the time domain response from the frequency domain parameters found in Nemoh. The solver considers several load contributions including the first order hydrodynamic loads composed of a contribution from excitation (Froude-Krylov and diffraction) and radiation force (added mass and damping). In addition, the hydrostatic force contribution is included. The frequency dependent excitation and radiation force coefficients are calculated in Nemoh from linear potential theory with the assumption of low wave steepness and small body motion amplitudes. The hydrostatic force is included as a linear spring term, again invoking the assumption of small body motions.

Furthermore, second order slow varying loads and viscous drag is considered. The slow varying drift forces (SVDF) are second order in wave amplitude, thus significantly smaller than the first order loads. Nevertheless, the drift forces have a significant role in the study of moored structures because their mean period lay in the lower frequency range, where the natural frequency of large structures is normally placed. While in regular wave, the drift forces are time invariant, in irregular wave the drift forces slowly vary in time. The exact solution of the second order diffraction problem is computational expensive, therefore, approximated solutions has been proposed to reduce the computational burden; the approximation proposed by Newman [19] is often regarded as a good trade off between accuracy and computational cost. In Orcaflex, the SVDF are implemented either using the full quadratic transfer function (QTF) or using the Newman approximation; this last has been used in the following work.

Finally, also wind and current loads are including through a drag formulation [16]. OrcaFlex calculates the drag at the instantaneous position, and calculates current and wind loads in all degrees of freedoms (DoFs). In addition, current and wind loads are included on the mooring lines using a Morison Approach [20].

2) Mooring Solver: The mooring solver in OrcaFlex is based on a lumped mass approach, where the mooring lines are discretized into a number of elements, and the mass, forces etc. are lumped into the nodes at the ends of each element. This approach is time efficient, but less accurate for e.g. snap loads. For more information see [21]–[23]. The accuracy of the mooring solver is highly dependent on the discretization of the lines, implying a balance between computational time and accuracy. In the present study, a convergence analysis was applied for securing a satisfying discretization.

C. Generalised Polynomial Chaos

A function with inputs subject to uncertainty can be mathematically expressed as $f(\mathbf{x}, Z)$, where $\mathbf{x}$ is the vector of deterministic input variables and Z is a random variable (variable subject to uncertainty). Z can take values in $\mathbb{R}$ from the set Ω of possible outcomes, and we write $Z : \Omega \to \mathbb{R}$. For such a process, *General Polynomial Chaos* provides a surrogate model to $f(\mathbf{x}, Z)$, based on a polynomial expansion:

$$f_{gPC}(\mathbf{x}, Z) = \sum_{k=0}^{\infty} \hat{f}_k(\mathbf{x})\psi_k(Z) \tag{5}$$

where $\hat{f}_k(\mathbf{x})$ are the polynomial coefficients and $\{\psi_k(Z)\}_{k=0}^{\infty}$ is the set of polynomial basis functions. For some statistical distributions with analytical representation, optimal convergence of the polynomial expansion is achieved by using the respective polynomials in the Wiener-Askey scheme [8].

Due to the practical impossibility of applying an infinite sum, Eq. (5) must be truncated at selected polynomial degree p:

$$f_{gPC}(\mathbf{x}, Z) \approx \sum_{k=0}^{p} \hat{f}_k(\mathbf{x})\psi_k(Z) \tag{6}$$

The required optimal degree must be defined by trial and error, until reaching sufficiently accurate results for the problem in question. A good indicator of the optimal polynomial degree is the evolution of the polynomial coefficients, $\hat{f}_k$. For smooth solutions, the value of the coefficients will decay rapidly as p increases, providing a good indication of when to truncate the expansion. As mentioned in the introduction, the mean and the variance of the output variables can be obtained from the the gPC coefficients $\hat{f}_k(\mathbf{x})$. More precisely, $\hat{f}_0(\mathbf{x})$ is a scaled value of the mean, and the variance can be obtained by summing the squares of the set of coefficients $\{\hat{f}_k(\mathbf{x})\}_{k=1}^{p}\}$ in the expansion.

In general, problems concerning uncertainty involve multiple random inputs. When dealing with the d

independent input random variables, $d \in \mathbb{N}$, $\psi(Z)$, instead of a single polynomial, gPC uses a tensor product of d polynomials, one for each variable, Eq. (6):

$$f_{gPC}(\mathbf{x},\mathbf{Z}) \approx \sum_{|\mathbf{k}|=0}^{p} \hat{f}_{\mathbf{k}}(\mathbf{x})\Psi_{\mathbf{k}}(\mathbf{Z}) = \\ = \sum_{|\mathbf{k}|=0}^{p} \hat{f}_{\mathbf{k}}(\mathbf{x})\psi_{k_1}(Z_1)\psi_{k_2}(Z_2)...\psi_{k_d}(Z_d) \quad (7)$$

where $\mathbf{Z} : \Omega \rightarrow \mathbb{R}^d$ is the vector of input random variables, $\mathbf{k} = (k_1, k_2, ..., k_d) \in \mathbb{N}_0$ $\mathbf{k}$ is a multi-index, $|\mathbf{k}| = k_1 + k_2 + ... + k_d$, and $\psi_{k_i}(Z_i)$ is the polynomial basis function of the variable Z_i, of degree k_i.

Beyond the general formulation presented above, gPC methods can be divided into two groups: Stochastic Galerkin Method and Stochastic Collocation Method. The Stochastic Galerkin Method is an intrusive method that requires the reformulation of the underlying equations that model a phenomenon. The Stochastic Collocation Method, on the contrary, is a non-intrusive method that only requires deterministic models to be run on specific points of the random sampling space. While the Stochastic Galerkin Method is more accurate in computing the gPC model, the reformulation of the underlying equations can be quite difficult. Moreover, in black-box models, such as commercial codes, it is generally impossible to apply the Stochastic Galerkin Method. Because of this, in this study we employed the Stochastic Collocation Method, which, although slower because it is built around and not into the solver, it is easier to apply in general, even for black-box codes.

For the computation of the gPC model $f_{\mathrm{gPC}}(\mathbf{x},\mathbf{Z}) \approx f(\mathbf{x},\mathbf{Z})$, we only need to post-process the results of simulations using the mathematical model at pre-selected values $\mathbf{z}^{(j)}$ of the uncertain input $\mathbf{Z}$. The points $\mathbf{z}^{(j)}$ where $f(\mathbf{x},\mathbf{Z})$ is to be evaluated depend on the method chosen to determine the coefficients $\hat{f}_{\mathbf{k}}$. For a process with dimension $d < 4$, the coefficients can be efficiently computed using the projection method. In applying this method, the coefficients $\hat{f}_{\mathbf{k}}(\mathbf{x})$ are determined by the inner product of $f(\mathbf{x},\mathbf{Z})$ with the polynomial basis, $\Psi_{\mathbf{k}}(\mathbf{Z})$, with respect to the probability density function (PDF) of the random variable, $\rho(\mathbf{Z})$, Eq. (8):

$$\langle \hat{f}_{\mathbf{k}}(\mathbf{x}), \Psi_{\mathbf{k}}(\mathbf{z}) \rangle = \frac{\int f(\mathbf{x},\mathbf{z})\Psi_{\mathbf{k}}(\mathbf{z})\rho(\mathbf{z})\mathrm{d}\mathbf{z}}{\int \Psi^2_{\mathbf{k}}(\mathbf{z})\rho(\mathbf{z})\mathrm{d}\mathbf{z}} \quad (8)$$

Equation (8) is solved using quadrature rules, such as Gauss quadrature, which provide the points $\mathbf{z}^{(j)}$ where the model is to be evaluated, and the quadrature weights, $\mathbf{w}^{(j)}$. For $d > 4$, the quadrature method becomes inefficient because, since multi-variable gPC is based on tensor product, the number of points $\mathbf{z}^{(j)}$ where the numerical model needs to be evaluated grows exponentially with the number d. In this case we would need to resort to other methods; however, in this study, $d = 2$, so we will employ the quadrature method.

The interaction between the different univariate polynomials in the tensor product can be controlled through the q-norm. A q-norm of 1 allows the tensor product of any set of univariate polynomials to reach the maximum selected polynomial order; decreasing the q-norm, until the minimum value of zero, decreases the maximum polynomial order allowed for products of univariate polynomials, reducing the total number of polynomial terms.

For the computation of the gPC model we used UQLab's version 1.0.0, Polynomial Chaos Expansions Module [24].

D. Model equations with random inputs

The uncertainty in the cable and hydrodynamic parameters is accounted for by introducing a set of random variables $\mathbf{Z} : \Omega \rightarrow \mathbb{R}^d$, which has been in shown [9]. The stochastic equation of motion for a perfectly flexible cable is, Eq. (9):

$$m_{\mathrm{l}}(s,\mathbf{Z})\frac{\partial^2 \mathbf{r}(s,t,\mathbf{Z})}{\partial t^2} = \left(\frac{\mathrm{T}\left(\epsilon(s,t,\mathbf{Z})\right)}{1+\epsilon(s,t,\mathbf{Z})}\frac{\partial \mathbf{r}(s,t,\mathbf{Z})}{\partial s}\right) + \\ + \frac{\partial}{\partial s} + \mathbf{f}_e(s,t,\mathbf{Z}), \quad (9a)$$

$$\epsilon(s,t,\mathbf{Z}) = \left|\frac{\partial \mathbf{r}(s,t,\mathbf{Z})}{\partial s}\right| - 1 \quad (9b)$$

where m_{l} is the mass per unit length, $\mathbf{r}(s,t,\mathbf{Z})$ is the position vector of a point s of the cable a time t, T is the tension magnitude, ϵ is the extension, and $\mathbf{f}_e(s,t,\mathbf{Z}$ is the vector of external forces acting on the cable. The stochastic Cummins equation is, Eq. (10):

$$\mathbf{M} + \mathbf{A}_\infty \ddot{\mathbf{x}}(t,\mathbf{Z}) + \int_{-\infty}^{t} \mathbf{K}(t-\tau)\,\dot{\mathbf{x}}(t,\mathbf{Z})\,\mathrm{d}\tau + \\ + \mathbf{C}\mathbf{x}(t,\mathbf{Z}) = \mathbf{f}_{\mathrm{ext}}(t) + \mathbf{f}_{\mathrm{moor}}(t,\mathbf{Z}) \quad (10)$$

where $\mathbf{M}$ is the generalised mass matrix of the floating structure, $\mathbf{A}_\infty$ is the added mass matrix at infinite frequency, $\mathbf{K}$ is the radiation impulse response function, $\mathbf{C}$ is the hydrostatic stiffness matrix, $\mathbf{f}_{\mathrm{moor}}$ is the mooring force vector, $\mathbf{f}_{\mathrm{ext}}$ is the vector of the remaining external forces acting on the floating structure, $\ddot{\mathbf{x}}$, $\dot{\mathbf{x}}$, and $\mathbf{x}$ are, respectively, the acceleration, velocity, and position of the floating structure, and t is time.

III. Case Study

The MSLWEC project [6], [7] has been using four large Danish ORECs as test cases for investigation, design and optimization of mooring solutions using a numerical model as described in section II-B. The present study considers one of the ORECs further: the Floating Power Plant P60 and the proposed mooring solution. In [7], the mooring system for the device was optimized to secure a high cost efficiency, while also fulfilling the design requirements in the design standard DNV-OS-E301 [2]. Earlier designs have considered chain catenary systems or polyester moorings, while the current layout focuses on highly compliant and more novel nylon ropes.

The present chapter describes the FPP, its deployment site and its optimized mooring system, which was proposed as a solution in [7]. The mooring system

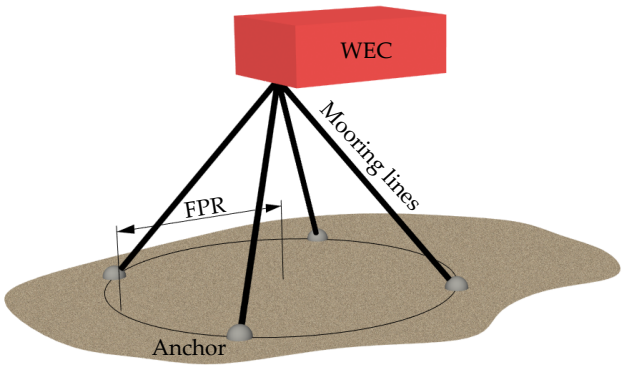

Fig. 2. Mooring concept applied to the P60. The system is a taut turret system with nylon lines.

does not resemble the final mooring layout for the FPP, but merely the solution from the MSLWEC project. Finally, the parameters considered in the reliability analysis is described.

E. Case - Floating Power Plant

The Floating Power Plant P60 is a combined wind and wave energy absorber, as illustrated in Fig. 1. The wave PTO is based on the principle of wave activated bodies (cf. [25]) through a number of pitching floaters. The mooring design is considering extreme events where the floaters are ballasted to have natural frequencies outside the wave spectrum so that the complete structure moves as one solid. Similarly, the wind turbine is in storm protection mode and is parked, meaning that a simple drag formulation can be used to estimate loads on it. The considered mooring system is a turret system with taut synthetic nylon lines as illustrated in Fig. 2, allowing the device to weathervane according to the incoming wave direction. Nylon ropes of the type Bridon Superline Nylon [26] are considered, with small chain segments located at the fairleads and anchors to allow for re-tensioning. The great advantage of nylon rope compared to chain and polyester is the high compliance, which reduces loads on the structure and in the lines. Studies, such as [27], illustrated how chain catenary mooring systems were inefficient for ORECs in shallow water depths, due to large wave-structure interaction and high mooring system stiffness. As a consequence, nylon lines were considered for the FPP P60, which provide significantly larger compliance.

The proposed mooring system for the P60 device was designed for deployment at the Belgian coast and for design conditions (100 year return period) presented in Table I. Both wind and current are modelled with vertically varying profiles as defined in design standards.

For the design in [7], the mooring system of the P60 was restrained to prevent surge motions from exceeding a certain design limit identified from the umbilical. Similarly, the pitch motions were limited according to the stability of the wind turbine and finally, the tensions in the lines were restrained according to the breaking strength given by the manufacturer,

TABLE I
ENVIRONMENTAL CONDITIONS USED FOR DESIGN OF OPTIMAL MOORING SYSTEM FOR THE P60 [7].

Environmental parameter	Design value
Significant wave height, H_s	6.55 m
Peak wave period, T_p	9.30 s
Wave Spectrum	JONSWAP, $\gamma = 3.3$
Current velocity, v_c	1.3 m/s
Ref. wind velocity, v_w	33.00 m/s
Wind spectrum	NPD-Spectrum
Water depth, h	30.00 m

TABLE II
OPTIMAL MOORING SYSTEM IDENTIFIED IN [7].

Mooring parameter	Optimum value
Footprint radius	40 m
No. of mooring lines	6
Mooring line diameter	192 mm
Mooring line mass (wet)	1.81 kg/m
Linearized axial mooring line stiffness	32,866 kN
Unstretched mooring line length	44.9 m
Minimum breaking strength	8240 kN
Maximum strain	25%

also considering safety factors from DNV-OS-E301. The optimization routine in [7] identified a mooring system as listed in Table II, considering a desire to obtain minimum lifetime cost. The optimization routine obtained the optimum by varying line type (diameter and axial stiffness) and mooring layout (number of lines and footprint radius).

IV. RELIABILITY ANALYSIS

F. Input Statistics

The parameters assumed to be uncertain were the water depth, the stiffness and breaking strength of the synthetic rope. The water depth was chosen because it has a natural variation due to tides and weather; the stiffness and strength of the synthetic rope were chosen because, due to their manufacturing process and natural degradation, synthetic materials show a large variability in their properties [28].

Because the stiffness and strength of the synthetic rope are significantly smaller than that of the chain, the chain is assumed to be rigid and unbreakable. Furthermore, we assume that the rope segments for each cable come from the same batch and, so, they have all the same stiffness and strength.

Since there are very little data available about the statistical distributions of the variables selected for analysis, we made assumptions based on published data and engineering judgement. First of all, the three input random variables – rope stiffness, rope breaking strength and water depth – are assumed to follow a normal distribution. To obtain the mean and standard deviation of the breaking strength of the synthetic rope, we used equations C.202 and C.203 on page 44 of [2], Eqs. (11) and (12) respectively,

$$S_c = \mu_s \left[1 - \delta_s \left(3 - 6\delta_s\right)\right], \text{for } \delta_s < 0.10 \quad (11)$$

$$S_c = 0.95 S_{mbs} \quad (12)$$

where S_c is the characteristic strength of the rope, μ_s is the mean value of the strength of the rope, δ_s is the

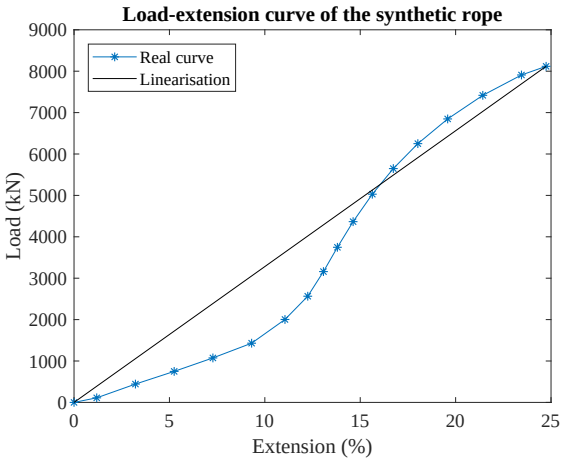

Fig. 3. Tension-elongation curved for a used synthetic fibre rope.

coefficient of variation of the strength of the rope, and S_{mbs} is the minimum breaking strength of the rope. These equations provide a model for the characteristic strength when the minimum breaking strength is known (usually provided by the rope manufacturer).

Combining Eqs. (11) and 12, assuming $\delta_s = 0.10$ for maximum variability, we can solve for μ_s. Knowing μ_s and the assumed value of $\delta_s = 0.10$, we obtain σ_s, the standard deviation of the strength of the rope.

Estimation of the distribution parameters for the rope stiffness was more *ad-hoc*, because we could not find any model for it. We assumed the mean stiffness, μ_{EA}, to be the linearised stiffness of a used synthetic rope, $EA_{\text{lin}} = 32.8656 \times 10^6 N$, computed from the load-elongation curve provided by the manufacturer, Fig. 3 [26]. To determine the standard deviation we assumed, as in Eq. (11), a coefficient of variation $\delta_{EA} = 0.10$, giving a standard deviation $\sigma_{EA} = 3.287 \times 10^6$ N.

Previous statistical analysis, described in [29], determined that, for a return period of 100 years, the extreme water depth variation is ± 5.5 m, meaning a 1% probability of occurrence. This probability was split between a positive and a negative variation: $0.5\,\%$ for a positive variation of more than 5.5 m and $0.5\,\%$ for a negative variation of more than 5.5 m.

We defined the mean water depth, μ_d, to be the design water depth, 30 m, Table II. To determine the standard deviation of the water depth, σ_d, we read from the standard normal distribution, Φ, the value with an exceedance probability of $0.5\,\%$, $Z = 2.58$, and applied the conversion from standard normal

$$\sigma_d = \frac{X - \mu_d}{Z} \tag{13}$$

where X represents maximum water depth, 35.5 m. The assumed and computed mean and standard deviation of the random input variables are listed in Table III.

G. Tension Statistics

The probability density function of the MPM tension, required to estimate the probability of failure of the mooring system, was determined using a *gPC* surrogate model. The input random variables to the *gPC* model of the MPM were the rope stiffness and water depth. Since these two variables are fully uncorrelated, they were represented by an independent copula. After convergence analysis, Fig. 5, we selected 5^{th} degree polynomials for the expansion, and a q-norm of 1. This required the evaluation of 36 different quadrature points, $\mathbf{z}^{(j)}$ (in other words, sets of rope stiffness-water depth values that were input into OrcaFlex).

To compute the probability density function of the MPM tension, we evaluated, in the gPC model, $1\,000\,000$ random values of rope stiffness and water depth, sampled from their respective distributions. Then, using the Kernel Density Estimation method, we smoothed the results to obtain the probability density function, Fig. 5. As can be seen, the MPM tension does not have a normal distribution: it is skewed to the right.

Figure. 5 also shows, for comparison, a histogram

TABLE III
PARAMETERS OF THE DISTRIBUTIONS OF THE VARIABLES OF INTEREST (DIST. - DISTRIBUTION; STD. DEV. - STANDARD DEVIATION).

Variable	Dist.	Mean	Std. Dev.
Rope strength	Normal	10.300×10^6 N	1.030×10^6 N
Stiffness	Normal	32.8654×10^6 N	3.287×10^6 N
Water depth	Normal	30 m	2.13 m

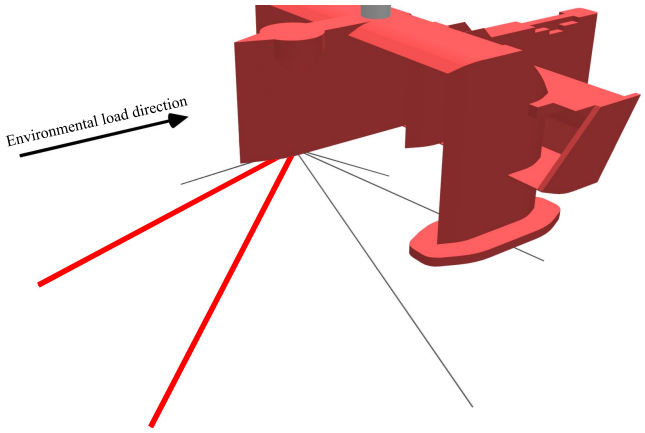

Fig. 4. Illustration of the line (red) considered in the present analysis.

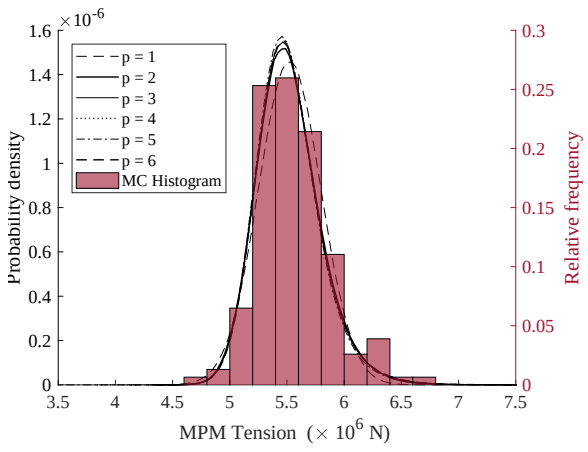

Fig. 5. Convergence of the probability density function for Most Probable Maximum tension in the most loaded cable.

TABLE IV
MEAN (μ_{MPM}) AND STANDARD DEVIATION (σ_{MPM}) OF THE NORMALISED DISTRIBUTION FOR THE MPM TENSION.

μ_{MPM}	σ_{MPM}
5.575×10^6 N	2.066×10^5 N

TABLE V
PROBABILITY OF FAILURE DISTRIBUTION AND RELIABILITY PARAMETERS.

Parameter	Value
μ_{F}	4.725×10^6 N
σ_{F}	1.051×10^6 N
β	4.498
P_{F}	3.426×10^{-6}

with the results of 154 Monte Carlo simulations using random inputs. Despite the number of simulations being too small to obtain converged statistical results using the the Monte Carlo method, the shape of histogram is already similar to the shape of the probability density functions for $p \geqslant 2$. On one hand, this partially validates the results of the gPC model; on the other hand, this shows the advantage of using gPC, which required only 36 simulations to obtain converged results, while using the MC method, 154 simulations are still not enough.

H. Reliability Estimation

As the MPM tension does not follow normal distribution, and we do not have an analytical expression for it, we applied the method described in [1] to obtain the mean, μ_{MPM}, and standard deviation, σ_{MPM}, of the normalised MPM tension distribution. The values obtained are listed in Table IV.

Using Eqs. (3) and (4), with μ_{MPM} and σ_{MPM} for the load, and μ_{s} and σ_{s} for the strength, we obtained the reliability index, β, and the probability of failure, P_{F}. These values are listed in Table V.

The most demanding reliability requirement listed in DNV-OS-E301 [2] is 1×10^{-5} for the ultimate limit state of a mooring system. With a probability of failure of 3.4×10^{-6} the mooring system for the FPP concept satisfies this requirement. In fact, the probability of failure is 10 times smaller than demanded by the in DNV-OS-E301. This shows some of the disadvantages of using deterministic over probabilistic design, which, in this case and even after optimisation, resulted in an over-design mooring system.

Renewable energy systems have relatively low profit margins, and their mooring systems account for a large portion of their cost, [30]–[32]. Strict design regulation, leading to over-designed components, can compromise their economic viability. For these structures, design regulations should properly account for the less severe consequences of mooring cable failure, perhaps by increasing the acceptable failure probability [31].

V. CONCLUSIONS AND FUTURE RESEARCH

We analysed the reliability of a mooring system designed in the MSLWEC project, using an offshore renewable energy converter as test case: the Floating Power Plant P60. Our analysis showed that the probability of failure of the mooring system is 3.4×10^{-6}, around an order of magnitude lower than the most demanding offshore Oil & Gas requirements. With a probability of failure lower than required, the mooring system is likely to be over-designed, and, therefore, more expensive than it needs to be. Moreover, the consequences of failure of the mooring system of an offshore renewable energy device are little to moderate, and the stringent design regulations of the offshore Oil & Gas sector might be too demanding, for a sector with small profit margins. This demonstrates need to develop appropriate design standards for offshore renewable energy, as current standards might lead to over-design.

Since there are not enough statistical data about loading and component strength in floating structures, we used numerical simulations to obtain the response of the converter under uncertainty in cable stiffness, cable strength and water depth. However, instead of applying the Monte Carlo Method, as it is common in reliability analysis, to run simulations on a PDE-based numerical model, we applied general Polynomial Chaos. Using general Polynomial Chaos, we built a surrogate model for the most probable maximum tension in the mooring cables as a function of random values of water depth and cable stiffness. The use of Polynomial Chaos reduced significantly the number of time-domain simulations required to obtain relevant statistics of the expected most probable maximum tension in the mooring cables: only 36 simulations required, whereas the Monte Carlo Method would require several hundreds or thousands of simulations. In fact, even after running 154 simulations using the Monte Carlo Method, it was not possible to obtain a stable histogram for the most probable maximum tension. Also, using polynomial chaos we were able to generate 1 000 000 random values for the most probable maximum tension, something that could hardly be done in an acceptable time-frame using Monte Carlo methods.

The analysis carried out is somewhat limited: several assumptions had to be made to estimate the parameters of the distributions of water depth, rope stiffness, and rope strength, and the validity of these assumptions might be questionable. Furthermore, only three design variables were judged to be uncertain. Several more parameters should be included in future studies concerning uncertainty: variability in wind, wave, and current loads; anchor positions; non-linear stiffness and submerged weight of the cables; and cable degradation as a function of depth and time. However, the most critical is the need for improved data on statistical distributions. While a better knowledge of the probability distribution of the water depth/tidal variation can be relatively easy to obtain (field measurements or forecasting), cable data is usually confidential. Improvement of probabilistic analysis and design of mooring systems requires publication of statistical data representative of mooring components, specially for synthetic cables, instead of using the assumed distributions presented in design codes, which might be too

conservative.

ACKNOWLEDGEMENT

We thank Floating Power Plant for making the data used in this study available.

REFERENCES

[1] V. Verderaime, "Illustrated structural application of universal first-order reliability method," NASA Marshall Space Flight Center, Huntsville, AL, Tech. Rep., 1994.
[2] DNV-GL, *Position Mooring*. DNV-GL Offshore Standard DNVGL-OS-E301, 2015.
[3] W. Brindley and A. P. Comley, "North sea mooring systems: How reliable are they?" in *Proceedings of ASME 2014 33rd International Conference on Ocean, Offshore and Arctic Engineering*, ser. Proceedings of ASME 2014 33rd International Conference on Ocean, Offshore and Arctic Engineering, San Francisco, California, USA, 2014.
[4] P. Thoft-Christensen and M. J. Baker, *Structural Reliability Theory and Its Applications*. Berlin, Heidelberg: Springer-Verlag, 1982.
[5] J. B. Thomsen, "Mooring solutions for large wave energy converters," Ph.D. dissertation, 2018.
[6] J. B. Thomsen, J. P. Kofoed, F. Ferri, C. Eskilsson, L. Bergdahl, M. Delaney, S. Thomas, K. Nielsen, K. D. Rasmussen, and E. Friis-Madsen, "On mooring solutions for large wave energy converters," in *Proceedings of the 12th European Wave and Tidal Energy Conference EWTEC2017*. Technical Committee of the European Wave and Tidal Energy Conference, 2017.
[7] J. B. Thomsen, F. Ferri, J. P. Kofoed, and K. Black, "Cost optimization of mooring solutions for large floating wave energy converters," *Energies*, vol. 11, no. 1, 2018, the article is published in a Special Issue of Energies, "Wave Energy Potential, Behavior and Extraction".
[8] D. Xiu and G. E. Karniadakis, "The Wiener-Askey polynomial chaos for stochastic differential equations," *SIAM Journal on Scientific Computing*, vol. 24, no. 2, pp. 619–644, 2002.
[9] G. Moura Paredes, C. Eskilsson, and A. P. Engsig-Karup, "Uncertainty quantification in mooring cable dynamics using polynomial chaos expansions," *Submitted Manuscript*, 2019.
[10] D. Bigoni, H. True, and A. Engsig-Karup, "Sensitivity analysis of the critical speed in railway vehicle dynamics," *Vehicle System Dynamics*, vol. 52, no. sup1, pp. 272–286, 2014. [Online]. Available: https://doi.org/10.1080/00423114.2014.898776
[11] J. P. Murcia, P.-E. Réthoré, N. Dimitrov, A. Natarajan, J. D. Sørensen, P. Graf, and T. Kim, "Uncertainty propagation through an aeroelastic wind turbine model using polynomial surrogates," *Renewable Energy*, vol. 119, pp. 910–922, 2018.
[12] O. P. Le Maître and O. M. Knio, *Spectral Methods for Uncertainty Quantification*, ser. Scientific Computation. Dordrecht: Springer Netherlands, 2010. [Online]. Available: http://link.springer.com/10.1007/978-90-481-3520-2
[13] D. Bigoni, A. P. Engsig-Karup, and C. Eskilsson, "Efficient uncertainty quantification of a fully nonlinear and dispersive water wave model with random inputs," *Journal of Engineering Mathematics*, vol. 101, pp. 87–113, 2016.
[14] E. Kreuzer and E. Solowjow, "Polynomial chaos and the heave motion of a cylinder in random seas," in *Proceedings in Applied Mathematics and Mechanics*, vol. 15. Springer, 2015, pp. 559–560.
[15] A. Babarit and G. Delhommeau, "Theoretical and numerical aspects of the open source bem solver nemoh," in *11th European Wave and Tidal Energy Conference (EWTEC2015)*, 2015.
[16] Orcina Ltd., "Orcaflex user manual," 2015.
[17] J. B. Thomsen, F. Ferri, and J. Kofoed, "Validation of a Tool for the Initial Dynamic Design of Mooring Systems for Large Floating Wave Energy Converters," *Journal of Marine Science and Engineering*, vol. 5, no. 4, 2017.
[18] W. Cummins, "The impulse response function and ship motions," David Taylor Model Basin Washington DC, Tech. Rep., 1962.
[19] J. Newman, "Second-order, slowly-varying forces on vessels in irregular waves," 1974.
[20] J. Morison, J. Johnson, S. Schaaf *et al.*, "The force exerted by surface waves on piles," *Journal of Petroleum Technology*, vol. 2, no. 05, pp. 149–154, 1950.
[21] M. Hall and A. Goupee, "Validation of a lumped-mass mooring line model with deepc wind semi-submersible model test data," *Ocean Engineering*, vol. 104, pp. 590–603, 2015.
[22] J. Davidson and J. V. Ringwood, "Mathematical modelling of mooring systems for wave energy converters: A review," *Energies*, vol. 10, no. 5, p. 666, 2017.
[23] J. B. Thomsen, F. Ferri, and J. P. Kofoed, "Screening of available tools for dynamic mooring analysis of wave energy converters," *Energies*, vol. 10, no. 7, 2017. [Online]. Available: http://www.mdpi.com/1996-1073/10/7/853
[24] S. Marelli and B. Sudret, "Uqlab user manual - polynomial chaos expansions," Chair of Risk, Safety & Uncertainty Quantification, ETH Zurich, Zurich, Tech. Rep., 2018.
[25] A. Pecher and J. Kofoed, *Handbook of Ocean Wave Energy*. Germany: Springer, 2017, vol. 7, this book is open access under a CC BY-NC 2.5 license.
[26] Bridon, *Wire and Fibre Rope Solutions*, 2016, [Online]. Available: http://www.bridon.com/uk/.
[27] J. B. Thomsen, J. P. Kofoed, M. Delaney, and S. Banfield, "Initial assessment of mooring solutions for floating wave energy converters," in *The Proceedings of the Twenty-sixth (2016) International Ocean and Polar Engineering Conference*, vol. 1. International Society of Offshore & Polar Engineers, 2016, pp. 590–596.
[28] N. Barltrop, *Floating Structures - A Guide for Design and Analysis, Volume 2*. Energy Institute, 1998.
[29] J. B. Thomsen, F. Ferri, and J. Kofoed, *Current Mooring Design in Partner WECs and Candidates for Preliminary Analysis: CM1 & M3*. Aalborg University, Department of Civil Engineering, 2016, confidential report.
[30] J. Fitzgerald, "Position mooring of wave energy converters," PhD Thesis, Chalmers University of Technology, 2009.
[31] G. M. Paredes, L. Bergdahl, J. Palm, C. Eskilsson, and F. T. Pinto, "Station keeping design for floating wave energy devices compared to floating offshore oil and gas platforms," in *Proceedings of the 10th European Wave and Tidal Energy Conference*. Aalborg, Denmark: European Wave and Tidal Energy Conference, 2013.
[32] L. Martinelli, P. Ruol, and G. Cortellazzo, "On mooring design of wave energy converters: the Seabreath application," in *Proceedings of the 33rd International Conference Coastal Engineering (ICCE)*, P. Lynett and J. McKee Smith, Eds., Santander, 2012, pp. 1–12.